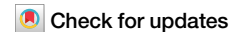


1

https://doi.org/10.1038/s44304-025-00106-2

River rejuvenation on a fluvial fan induced by typhoons and earthquakes



Jui-Yi Ho¹ ⊠, Wei-Lin Lee¹, Che-Hsin Liu¹, Naoki Sakai², Yi-Chin Chen³, Chih-Hsin Chang¹ & Hongey Chen¹

This study investigates decadal-scale river rejuvenation and migration in Taiwan's Mu-Gua River watershed, influenced by typhoons and earthquakes. Typhoon Ofelia (1990) caused rapid sediment aggradation and channel instability, leading to severe damage and the relocation of Tung-Men Village. Analysis of historical hydrological and topographic data reveals that such extreme events accelerate riverbed incision and channel migration, disrupting fluvial equilibrium. Post-earthquake observations indicate heightened sediment transport during high-flow events within three years of seismic activity, while low-flow conditions show negligible differences. These findings underscore the profound influence of compound natural hazards on river morphology and community safety, highlighting the necessity of integrating geomorphic insights into disaster risk reduction and land-use planning.

As a river evolves from its youthful stage to maturity and old age, it may encounter external forces that cause abrupt changes in its base level of erosion¹. These changes disrupt the equilibrium of fluvial processes, resulting in intensified erosion and sediment redistribution. Consequently, landforms typical of young rivers may reappear in landscapes previously dominated by mature or old-age features. This process is known as river rejuvenation². In fluvial geomorphology, river rejuvenation is characterized by enhanced vertical incision, increased flow velocity, and notable changes in river morphology³. These modifications disturb the river's dynamic equilibrium and influence adjacent landscapes, often resulting in the formation of new sedimentary layers and increased occurrences of geological hazards. The timescale of river rejuvenation varies depending on regional geological conditions, climate, tectonic activity, and river characteristics, ranging from several decades to thousands of years⁴.

The impacts of typhoons and earthquakes on river migration have gained increasing attention in recent years. These extreme natural events can trigger substantial sediment influx, channel scouring, and lateral erosion over short timescales, leading to significant alterations in river morphology and disruption of dynamic equilibrium. For instance, intense rainfall during typhoons often causes landslides and debris flows^{6–8}, introducing large volumes of sediment into river systems, which can result in aggradation, widening, or altered flow paths. Similarly, strong earthquakes often trigger large-scale coseismic landslides in mountainous regions^{9,10}, influencing long-term erosion and landscape evolution¹¹. When occurring sequentially or concurrently, typhoons and earthquakes can have cumulative impacts. Therefore, integrating long-term monitoring data, topographic analysis, and hydrological modeling is essential to better understand river evolution

under such compound disturbances and to support disaster risk reduction and watershed management.

The evolution of river morphology across decadal to centennial timescales is highly complex ^{12,13}. Taiwan, located at the oblique convergence zone between the Philippine Sea Plate and the Eurasian Plate, is characterized by frequent seismic activity and steep terrain. Additionally, Taiwan lies in the primary path of western Pacific typhoons and within a tropical monsoon climate zone, leading to high annual rainfall. These conditions result in rivers that are steep, fast-flowing, and prone to rapid sediment mobilization ^{14,15}. Consequently, Taiwan serves as a natural laboratory for studying fluvial geomorphic processes ^{16,17}. For example, Cook et al. ¹⁸ documented the aftermath of the 1999 Chi-Chi earthquake, where the riverbed of the Daan River rose by up to 10 meters ¹⁸. Subsequent erosion led to the formation of a 20-meter-deep gorge, projected to be fully eroded within 50 years through downstream sweep erosion. This case illustrates the rapid rates of geomorphic change observed in Taiwan's dynamic landscape.

Typhoons, heavy rainfall, and earthquakes often trigger landslides and debris flow. For instance, on June 23, 1990, Typhoon Ofelia brought heavy rainfall to the Tung-Men area of the Mu-Gua River in Hualien County, resulting in severe debris flow. This event led to 39 fatalities, left 68 people homeless, and caused the complete destruction of 24 houses, with 11 houses being partially destroyed. The disaster caused significant casualties, had a major social impact on Taiwanese society, and became the first documented instance in Taiwan where an entire village was relocated because of a disaster 19,20. More than 30 years later, the present study used long-term records from the watershed, including landslide ratios, rainfall, runoff, sediment transport, river cross-sectional data, and earthquake records, to investigate the interactions among climate, seismic events, and river

¹National Science and Technology Center for Disaster Reduction, New Taipei City, 231007, Taiwan. ²National Research Institute for Earth Science and Disaster Resilience, Ibaraki, 3050006, Japan. ³Department of Geography, National Changhua University of Education, Changhua City, 500207, Taiwan.

e-mail: juiyiho@ncdr.nat.gov.tw

rejuvenation processes. Through this approach, the present study provided a detailed analysis of river rejuvenation processes.

Results

As shown in Fig. 1, the Mu-Gua River originates from the Chi-Lai and Neng-Gao mountain ranges and flows southeastward toward Tung-Men Village, transitioning from mountainous terrain to alluvial plains before merging with the Hua-Lien River. The steep topography on the eastern slope of Chi-Lai Mountain has been shaped by three major tectonic events during the orogenic evolution of the Mu-Gua River Valley.

The watershed's geology is primarily composed of Ta-Nan-Ao Schists, which include phyllite and metamorphosed limestone. In addition, the active Ling-Ding Fault crosses the confluence of the Mu-Gua and Hua-Lien Rivers, contributing to the region's complex geomorphic structure. The overall topography forms an inverted triangular shape, with Chi-Lai Mountain at its apex, characterized by steep slopes and rapid flow velocities. The upstream watershed is relatively wide, while the downstream section narrows, promoting the accumulation of substantial surface runoff.

The watershed elevation ranges from 20 to 2607 meters and encompasses a drainage area of 457 km², with an average slope of 0.053. Several rainfall monitoring stations are located within the watershed, including the Tung-Men Weather Station (Central Weather Bureau; E: 121°29'34.2", N: 23°57'56.5"), Long-Jian Station (E: 121°24'40.7", N: 24°01'23.5"), and Hualien Station (E: 121°36'17", N: 23°58'37"). According to historical rainfall records, the region receives an average annual precipitation of approximately 2050 mm, distributed over about 152 rainy days per year.

The Ren-Shou Bridge flow station, established in 1960, provides long-term hydrological records on discharge, water levels, and sediment concentrations. The upstream catchment above Ren-Shou Bridge covers 426 km², with a main channel length of ~4.78 km and an average riverbed gradient of 1:90. Due to its steep and high-relief terrain, the middle and lower reaches of the river are highly susceptible to deep channel incision during flood events. During typhoon and flood periods, the maximum daily discharge can reach 1997 m³/s, while the peak instantaneous discharge may exceed 4160 m³/s—nearly 200 times the average base flow. These extreme hydrological conditions allow for rapid surface runoff and sediment transport, enabling material to exit the watershed and reach the ocean over very short spatial and temporal scales.

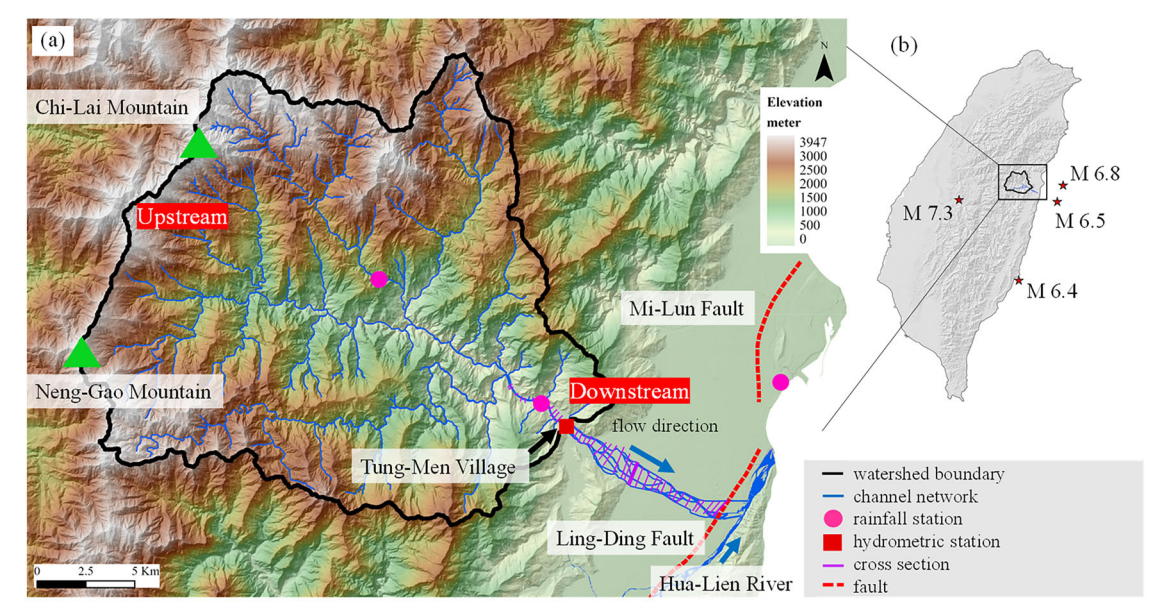
As shown in Fig. 2, Typhoon Ofelia, on June 23, 1990, brought heavy rainfall, which triggered severe debris flows in multiple tributary streams²¹.

These flows led to the accumulation of large amounts of sediment in the mainstream of the Mu-Gua River, causing the riverbed to rise. This elevation of the riverbed resulted in a lowering of the base level of erosion, thereby increasing the river's erosive capacity when the river gradient steepened once again. This process led to the rejuvenation of the Mu-Gua River's fluvial geomorphology, causing the river to revert to characteristics typical of a younger stage. Over the past few decades, river rejuvenation and incision processes have remained key topics in geomorphological research. For this study, we collected cross-sectional survey data from the Mu-Gua River at five intervals following Typhoon Ofelia, specifically data from the years 1993, 2008, 2011, 2016, and 2021, to investigate the evolution of the river rejuvenation processes (Fig. 3).

When the changes in erosion and deposition from 1993 to 2021 were presented as a quartile plot (Fig. 4), the cross-sectional measurement data indicated that most of the cross-sections exhibited downward incision during this period, with the maximum of average incision depth reaching 5.5 m. The most pronounced incision occurred during the period from 1993 to 2008, primarily due to the river rejuvenation triggered by Typhoon Ofelia (1990). Between 2008 and 2021, the dynamic equilibrium of riverbed erosion and deposition exhibited relative stability, with only minor changes observed between 2011 and 2016.

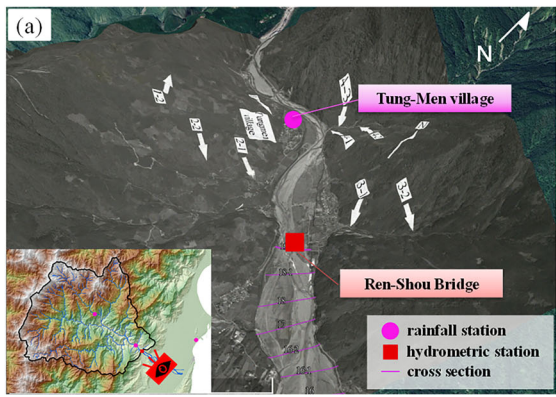
A comprehensive analysis of the river migration of the river center for each period and cross-section was also conducted. The comparison of five intervals over 29 years, from 1993 to 2021, showed that the maximum left-bank migration reached 777.9 m, while the maximum right-bank migration reached 324.4 m. During the 16-year period from 1993 to 2008, the maximum left-bank migration was 932.4 m, and the maximum right-bank migration was 416.18 m, marking this as the period with the most significant river center movement and the most intense incision. The trend of river migration generally aligns with the patterns of dynamic equilibrium of riverbed erosion and deposition between 1993 and 2021.

The present study further collected long-term daily discharge data to investigate the effect of daily discharge on riverbed erosion and deposition. An analysis revealed that the maximum daily discharge recorded at the Renshou Bridge flow station from 1993 to 2021 reached 1997 m³/s, with an average daily discharge of 9.33 m³/s. From 1993 to 2008, when riverbed incision was most severe, the maximum daily discharge was 1277 m³/s, and the average daily discharge was 8.11 m³/s, indicating no significant difference compared with the discharge levels recorded in other years.



 $\label{lem:condition} \textbf{Fig. 1} \ | \ \textbf{The location of the Mu-Gua River. a} \ \text{The river originates from the Chi-Lai} \ \text{and Neng-Gao Mountains and flows southeast through Tung-Men Village before joining the Hua-Lien River. Major faults, including the Ling-Ding and Mi-Lun Faults.}$

The watershed ranges in elevation from 20 to 2607 m and features rapid runoff. Key monitoring stations, channel networks, and cross-section locations are shown. **b** The inset map indicates nearby earthquake epicenters ($M \ge 6.4$) from 1990 to 2022.



23, 1990. a Pre-event conditions showing the location of Tung-Men Village, Ren-

Shou Bridge, rainfall and hydrometric stations, and surveyed cross sections. b Post-

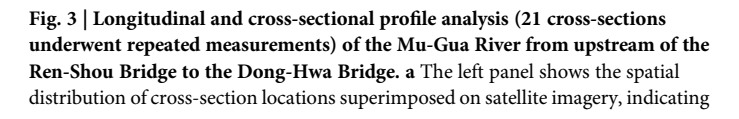
Fig. 2 | Satellite imagery showing the sedimentation and fluvial impact area of the Mu-Gua River near Tung-Men Village before and after Typhoon Ofelia on June trigger

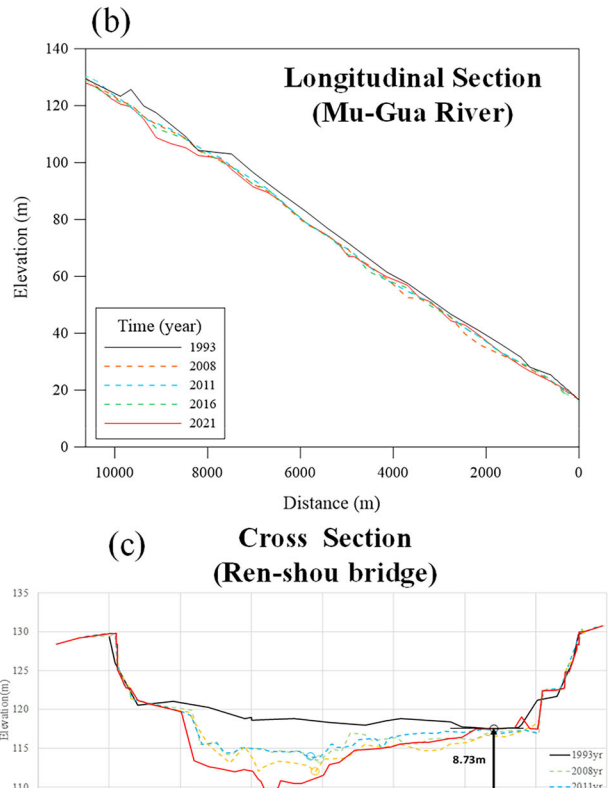
Tung Men village

Ren-Shou Bridge

event imagery indicating the sediment accumulation caused by severe debris flows triggered by Typhoon Ofelia. These flows raised the riverbed elevation and increased the river's erosive power, initiating a process of river rejuvenation. (after Chen, 2006)²¹.







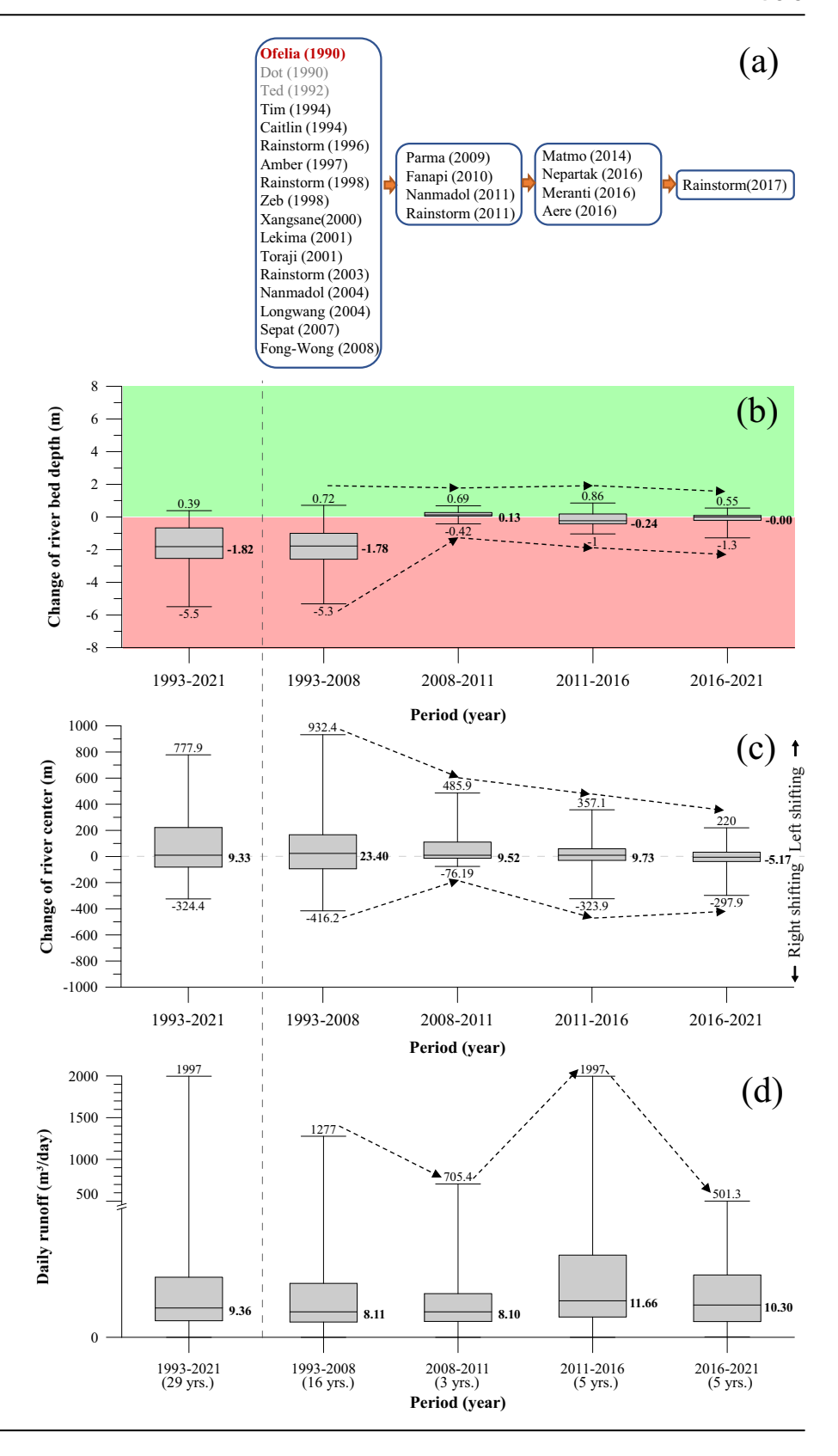
the reach used for morphological analysis. **b** Longitudinal profile changes from 1993 to 2021 reveal a general trend of riverbed incision along the Mu-Gua River. **c** Cross-sectional profiles at the Ren-Shou Bridge illustrate significant riverbed incision from 1993 to 2021.

Between 2011 and 2016, the maximum daily discharge again reached 1997 m³/s, with an average daily discharge of 11.63 m³/s, which was the highest among all the investigated periods. However, this only resulted in a slight additional incision of the average riverbed elevation and a minor increase in river migration. These findings suggest that the river rejuvenation of the Mu-Gua River, triggered by Typhoon Ofelia, led to changes in the erosion and deposition patterns of the river, prompting the river to adapt to seek a more stable state. Regarding discharge levels or sediment transported

from upstream, the river formed a stable river morphology and gradient, a process known as dynamic equilibrium. With the continuous scouring of the Mu-Gua River riverbed, the overall erosion and deposition variations, along with the lateral shifts of the river center, tended toward stabilization.

In addition, according to cross-sectional survey data from 1993 and 2008 (spanning a 16-year period), the Mu-Gua River experienced numerous typhoons and heavy rainfall events as show in Fig. 4 that caused significant downcutting and lateral migration of the river. Over time, the river gradually

Fig. 4 | Box plots illustrating changes in riverbed elevation and river center migration of the Mu-Gua River (21 cross-sections underwent repeated measurements) across four time intervals: 1993-2008, 2008-2011, 2011-2016, and 2016-2021. a Major typhoon and heavy rainfall events (daily rainfall depth >250 mm) during four periods after Typhoon Ofelia (1990) b Vertical axis represents changes in riverbed elevation (in meters), with negative values indicating incision and positive values indicating deposition. The median incision was most pronounced during the 1993-2008 period, with a maximum average incision depth of -5.5 m, attributed to river rejuvenation following Typhoon Ofelia (1990). From 2008 to 2021, riverbed elevation changes diminished, reflecting a trend toward dynamic equilibrium. c Lateral migration of the river center during the same periods, where values to the right of the dashed line indicate right-bank migration and those to the left indicate left-bank movement. The most significant river migration occurred from 1993 to 2008, with reduced migration observed in later periods. d Annual statistics of daily discharge from the Ren-Shou Bridge flow station. The maximum daily discharge peaked at 1997 m3/s, and average daily discharge increased slightly over time.



approached a state of dynamic equilibrium between erosion and deposition. This study further incorporates analysis using the daily flow duration curve. The daily flow duration curve is a hydrological method used to describe the characteristics of a watershed by presenting the probability of flows exceeding various intensity levels over a given period. It is created by arranging the daily discharge data, from highest to lowest. The exceedance

probability for each flow value is then calculated, and the relationship between flow magnitude and exceedance probability is plotted. The resulting curve reflects the variability and distribution of flow intensity, providing valuable insights into the frequency of high-flow and low-flow events in the watershed^{22,23}. When the discharge corresponds to low exceedance probabilities on the daily flow duration curve, it indicates the

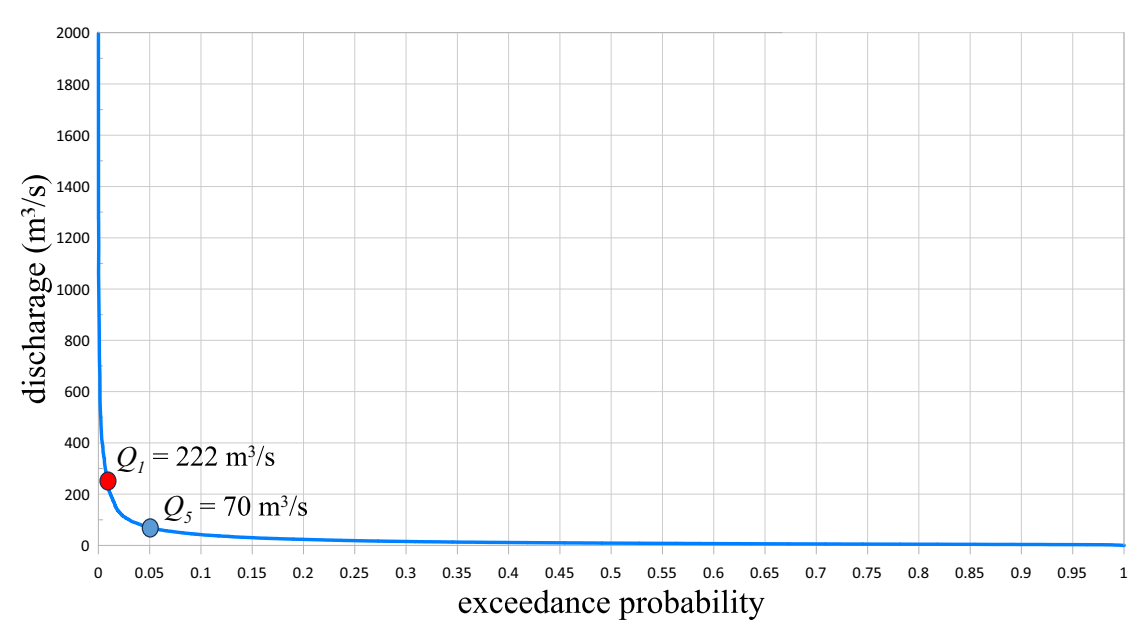
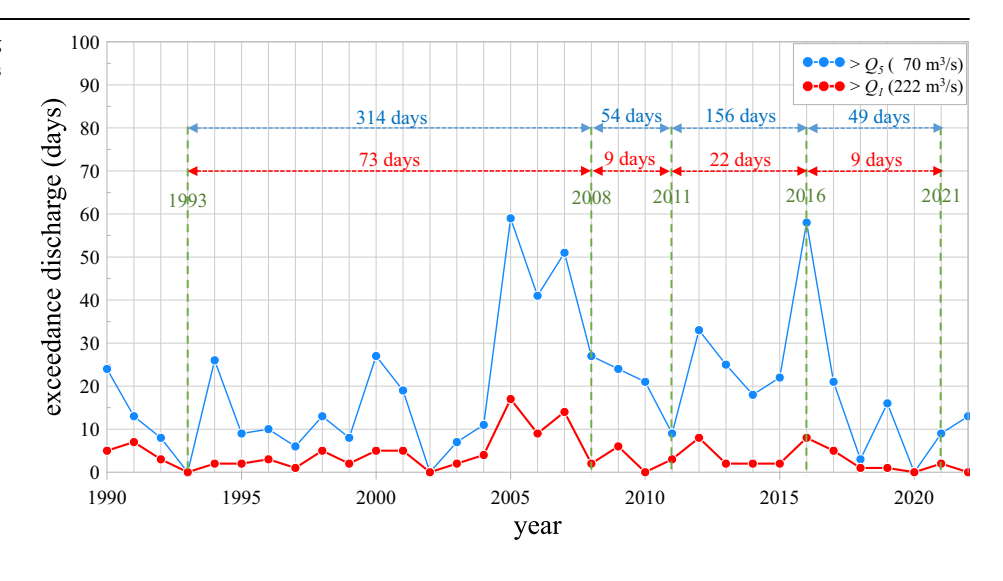


Fig. 5 | Daily flow duration curve (1990–2022) from the Ren-Shou bridge flow station in Mu-Gua river. From daily flow duration curve, the discharge values corresponding to exceedance probabilities of 1 and 5% were determined to be Q_1 is 222 m³/s and Q_5 is 70 m³/s.

Fig. 6 | Number of days with discharges exceeding the high discharge. Number of days with discharges exceeding Q_I (red line) and Q_5 (blue line) for each year from 1990 to 2022, along with the cumulative totals for the periods 1993–2008, 2008–2011, 2011–2016, and 2016–2021.



occurrence of flood events or high flows, which have substantial impacts on river morphology. Floods transport large quantities of sediment, causing both erosion and river migration. Daily discharge data from 1990 to 2022, recorded at the Ren-shou Bridge flow station on the Mu-Gua River, were used to construct the daily flow duration curve (as shown in Fig. 5). From the curve, the discharge values corresponding to exceedance probabilities of 1 and 5% were determined to be Q_I is 222 m³/s and Q_5 is 70 m³/s, respectively. Both thresholds were then used to calculate the number of days with discharges exceeding Q_I and Q_5 in the following periods: 1993–2008, 2008–2011, 2011–2016, and 2016–2021.

The results show that the period from 1993 to 2008 had the highest frequency of high-flow events, with 73 days exceeding Q_I and 314 days exceeding Q_5 . Corresponding cross-sectional data from this period indicate significant river migration. The second highest was the 2011–2016 period, with 22 days exceeding Q_I and 156 days exceeding Q_5 , during which moderate erosion and river shifts were observed. In contrast, the other two periods had very few high-flow days, and the corresponding cross-sectional data indicated a relatively stable river with near-equilibrium conditions in

sediment transport. These results are consistent with the river migration observed in the cross-section surveys (Fig. 6), thereby establishing a clear linkage between daily discharge characteristics and river migration in the Mu-Gua River. This analysis of the river's geomorphological and hydrological evolution contributes to the understanding of decadal-scale river changes and the process of river rejuvenation.

The present study collected data on the historical seismic events that occurred after Typhoon Ofelia (September 1990) and affected the Mu-Gua River watershed between 1990 and 2022, including the Hualien Earthquake on December 13, 1990 (magnitude 6.5, depth 2.82 km), the Chi-Chi Earthquake on September 21, 1999 (magnitude 7.3, depth 8 km), and the Cheng-Kung Earthquake on December 10, 2003 (magnitude 6.4, depth 17.7 km), the Hualien Earthquake on February 6, 2018 (magnitude 6.2, depth 6.3 km), and the Hualien Earthquake on April 18, 2019 (magnitude 6.3, depth 18.8 km). The study analyzed long-term daily records of rainfall, river discharge, daily sediment transport rates, landslide ratios, and the timing of major seismic events in the Mu-Gua River watershed from 1990 to 2022 to investigate hydrological and geomorphological changes within the watershed.

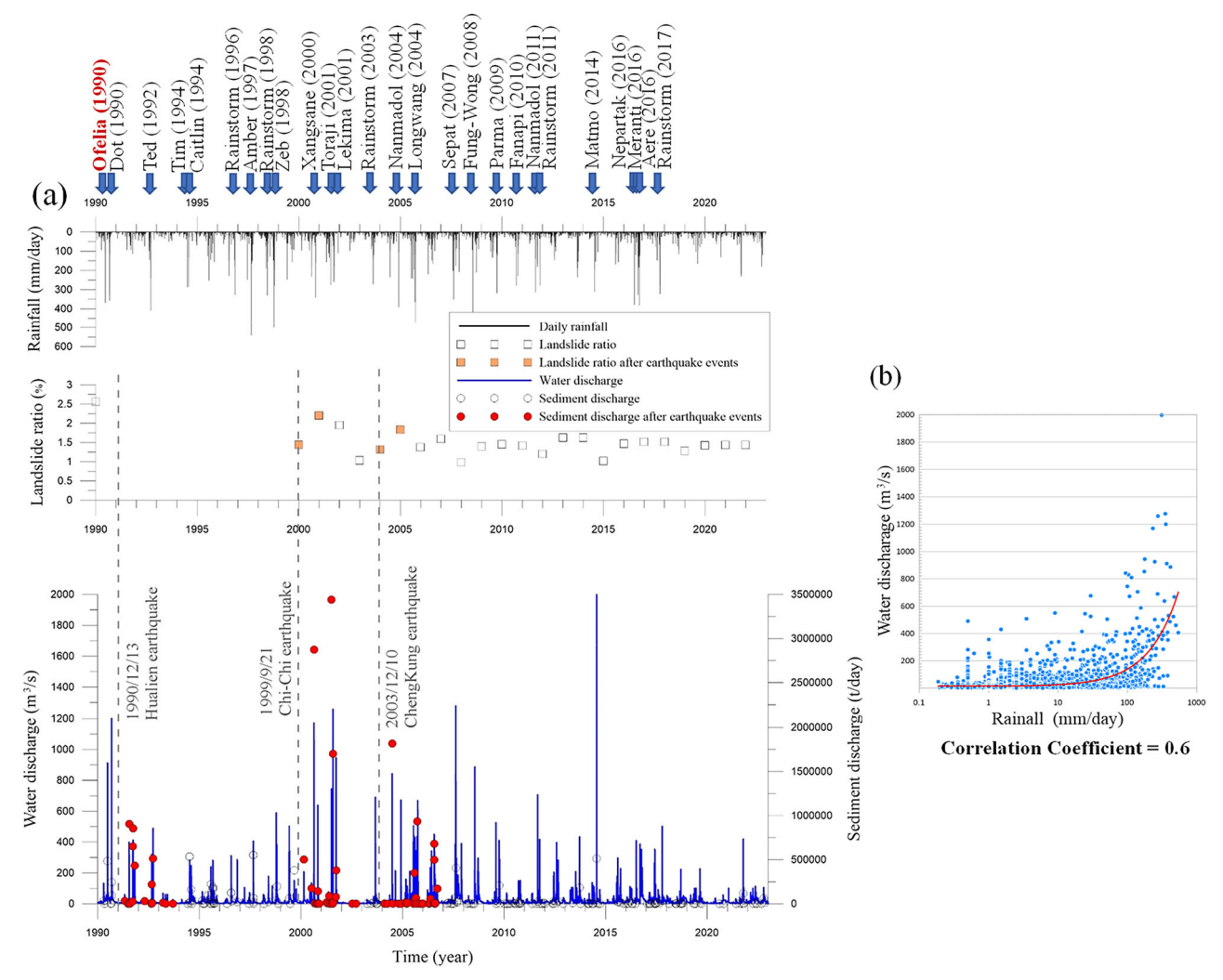


Fig. 7 | Daily rainfall, landslide ration, water discharge, sediment discharge, and earthquake events in Mu-Gau River from 1990–2022. a Annual trends of daily rainfall, river discharge, and sediment transport in the Mu-Gua River watershed, with annotations of major earthquake events. The black line at the top shows annual daily rainfall, the blue line represents daily discharge (m³/s), and the red dots indicate sediment discharge observations. The lower panel presents the annual landslide ratio (%) in the watershed (gray boxes), with red squares highlighting years affected by

major seismic events: the 1990 Hualien Earthquake, the 1999 Chi-Chi Earthquake, and the 2003 Chengkung Earthquake (marked with vertical dashed lines). A clear increase in sediment transport is observed following each seismic event, particularly within 1–3 years post-earthquake. The results demonstrate that post-earthquake sediment transport intensifies during high-flow events and gradually returns to normal conditions approximately three years after the earthquake. **b** Daily rainfall and water discharge have a positive correlation (correlation coefficient is 0.6).

As depicted in Fig. 7, an analysis of the annual landslide ratio in the watershed revealed an increasing trend following major seismic events. For example, in the 1 to 2 years after the 1999 Chi-Chi Earthquake, the landslide ratio in the watershed rose from 1.4 to 2.2%. Similarly, after the 2003 Chengkung Earthquake, the landslide ratio increased to 1.8% in the 1 to 2 years following the event. In the third year after the earthquake, the landslide ratio began to decline. By contrast, from 2006 to 2022, when no major seismic events occurred, the landslide ratio ranged between 1.0 and 1.6%, with an average value of 1.4%. These findings indicate that the increase in landslide ratios within the Mu-Gua River watershed persisted for $\sim\!\!2$ years after an earthquake, with an increase ranging from 0.4 to 0.8%.

As indicated by the daily rainfall and river discharge observation data from the Ren-Shou Bridge station (Fig. 3), there was a positive correlation (correlation coefficient is 0.6) between daily rainfall (black line) and daily discharge (blue line) as show in Fig. 7. This correlation was primarily due to the heavy rainfall during typhoon events in the Mu-Gua River watershed, which generated substantial surface runoff, potentially increasing sediment transport. However, the figure does not indicate a strong positive correlation between daily discharge and sediment transport data. As shown in Fig. 7, significant increases in sediment transport were recorded following the

Hualien Earthquake in 1990, the Chi-Chi Earthquake in 1999, and the Cheng-Kung Earthquake in 2003, indicating a clear relationship between increased sediment transport and earthquake events. According to Fig. 8, during low-flow conditions (discharge <50 m³/s), sediment transport data within 3 years post-earthquake indicated no differences compared with normal periods. Nevertheless, during high-flow conditions, sediment transport levels were significantly higher during the 3-year period following a major earthquake than during regular periods. After an earthquake, the slopes within the watershed became unstable, loosening soil and sediment. With subsequent rainfall events and the concentration of surface runoff, the sediment particles gradually transitioned from a static to a mobilized state, moving downstream with the surface runoff. When the unstable soil and sediment continued to be released after an earthquake, the sediment transport rates in the watershed typically returned to normal conditions after ~3 years. The analysis of hydrological and sediment observation data from the Ren-Shou Bridge station provides clear scientific evidence of this phenomenon.

Discussion

River rejuvenation refers to the reactivation of vertical erosion in a river system, often caused by abrupt changes in the river's base level triggered by

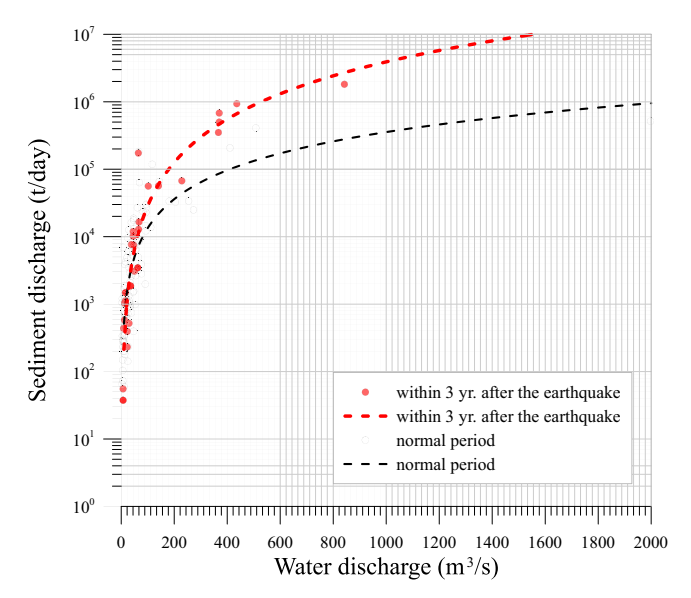


Fig. 8 | The relationship between sediment transport and daily discharge from Ren-Shou bridge flow station in the Mu-Gua River, comparing post-earthquake periods (within 3 years after major earthquakes) with normal periods. Red markers and dashed lines represent post-earthquake conditions, while black markers and dashed lines represent normal conditions. During high-flow events, sediment transport was significantly higher in the 3 years following major earthquakes, due to increased sediment availability from unstable slopes. This effect diminished over time, with sediment transport returning to normal levels ~3 years after each event.

external forces. These changes lead to shifts in erosion and sediment deposition processes, forming youthful geomorphic features in regions typically characterized by mature or old-age landscapes. Traditionally, geomorphological studies have emphasized long-term fluvial evolution, while short-term and decadal-scale river dynamics remain less explored due to their rapid and complex nature.

Taiwan, located at the oblique convergence of the Philippine Sea Plate and the Eurasian Plate, experiences frequent seismic activity and intense rainfall from Pacific typhoons. These conditions produce steep terrain and fast-flowing rivers, making Taiwan an ideal natural laboratory for studying fluvial geomorphology. This study investigates the Mu-Gua River watershed, focusing on the impacts of typhoons and earthquakes on riverbed incision, sediment transport, and channel migration. Historical datasets on rainfall, discharge, sediment load, and cross-sectional profiles were analyzed. The results reveal that Typhoon Ofelia (1990) initiated river rejuvenation, increasing sediment mobilization and river incision. Over the following decades, the river gradually approached a dynamic equilibrium, with erosion and deposition processes stabilizing.

To clarify the relationship between landslides, earthquakes, and sediment discharge, the answer can be also drawn from the understanding of landslide-triggered sediment mobilization and the role of rainfall-runoff processed and sediment transportation. While earthquakes significantly increase the production of sediment by triggering landslides, the subsequent sediment discharge is not solely due to the seismic events but rather the ability of heavy rainfall to mobilize and transport these materials during flood events^{24,25}. After major earthquakes, the production of loose sediment from landslides sharply increases. This newly generated sediment, however, needs strong runoff from intense rainfall during typhoon events or heavy storms to be transported downstream. Sediment discharge spikes during the high-discharge periods following earthquakes because the river's sediment load is elevated. As rainfall intensity increases, more sediment is mobilized from these landslides and carried away by the river's fast flow.

However, after a few years, once the earthquake-triggered landslides have depleted the available sediment in the watershed, further heavy rainfall events no longer result in increased sediment discharge, as the riverbed has already been cleared of the loose material. Sediment discharge decreases

even during heavy rain, because the river no longer has enough mobilizable material from the landslides. This process explains why post-earthquake sediment discharge may be initially high but later stabilizes, regardless of rainfall intensity.

Specifically, this study indicates that river incision and migration can lead to the destruction of riverbank structures (such as bridge pier scour and embankment failures), severe flooding disasters, and environmental degradation. Furthermore, we elaborated on the Typhoon Ofelia (1990) event, where rapid sediment aggradation and subsequent channel instability resulted in significant damage to Tung-Men Village, ultimately leading to the relocation of the entire community. This case highlights the close relationship between geomorphic changes and disaster risk, underscoring the importance of incorporating knowledge of compound natural hazards into disaster prevention and land-use planning. Furthermore, hydrological data show that post-earthquake sediment transport during high-flow events was significantly higher within 3 years after seismic activity, whereas differences were negligible under low-flow conditions. These findings contribute to the understanding of decadal-scale river evolution under compound climatic and tectonic forcing.

Methods

Monitoring data from the Taiwan Water Resources Agency (WRA) detail river cross-section surveys conducted along the Mu-Gau River at intervals of roughly 0.5 km (Figs. 1, 3), in compliance with Taiwanese governmental standards²⁶. Of the surveyed locations, 21 cross-sections underwent repeated measurements between 1993 and 2021. Steel or concrete markers anchor both ends of each cross-section, with their positions accurately determined via benchmarks and GPS systems. The elevation control for these measurements follows the 2001 Taiwan Vertical Datum System (TWVD2001), using first and second-order benchmarks or water-level control points certified by relevant authorities. Horizontal coordinates are derived using the latest legal coordinate system announced by the Ministry of the Interior, ensuring precision up to millimeter accuracy. For measurement of crosssections, techniques such as total station and GNSS positioning are employed to ensure high accuracy in capturing riverbed and bank profiles. In terms of error checks, horizontal measurements should exhibit an accuracy of no more than 3 cm, and vertical errors for the cross-section benchmarks should be less than 5 cm. The discrepancies between the observed distances and the known coordinates of reference points should not exceed 1/5000 of the measurement distance, ensuring the precision and reliability of the data²⁷.

To assess the fluvial discharge and sediment transport dynamics of the Mu-Gua River, hydrometric data from the Ren-Shou Bridge flow station (H0190H01) were acquired from the Taiwan Water Resources Agency's Hydrological Yearbooks, covering the period 1990–2021²⁸. Daily discharge measurements were recorded, while suspended sediment concentrations were determined from 30 samples collected annually using the DH-48 depth-integrating sampler. Calibration of the sampling process was conducted each year by the Taiwan Water Resources Agency to maintain data reliability. In the suspended sediment sampling process, it is essential that the water sample collected by any sampler represents the concentration of sediment at the measurement point. Therefore, the flow velocity at the sampler's intake should match the water flow velocity, and the intake should be directed downstream to accurately represent the average sediment content along the vertical line. The sampling duration is set to 10 s to ensure an average value within that timeframe. Each sample should occupy ~3/4 of the volume of the water sample bottle to prevent overflow and ensure accuracy. The diameter of the intake pipe is adjusted based on the size of the sediment particles being sampled, ensuring the intake velocity equals the flow velocity. During full-depth sampling, a 0.318 cm diameter intake is used for regular water depths, and a 0.635 cm diameter intake is used for shallow waters.

In turn to the methodology about the detection of landslide, the Mu-Gua River watershed's data is sourced from the Water Resources Agency, the Geological Survey and Mining Management Agency, and the Agency of Rural Development and Soil and Water Conservation. The island-wide landslide detection process primarily utilizes SPOT satellite imagery

(SPOT-6/7), with a spatial resolution of 1.5 meters, to map landslides across the entire island^{29–33}. These images are carefully selected based on factors such as optimal cloud cover and viewing angles to maximize the accuracy of landslide detection. The methodology includes multiple stages: First, precise data calibration and alignment are ensured. Color adjustments correct frequency deviations to align images with natural colors. Automatic radiometric correction ensures consistent image quality across datasets. Color fusion processing and SSIM (Structural Similarity Index) color fusion enhance image accuracy and visual quality. Multi-temporal image registration ensures proper alignment over time, while image enhancement processing improves clarity. Geometric and radiometric corrections maintain overall accuracy and consistency. The methodology concludes with super-resolution image enhancement, increasing resolution and detail for high-quality analysis. The approach also accounts for the limitations of image acquisition dates, acknowledging that the imagery may not fully capture the impacts of all disasters over a given year.

Data availability

The data about daily rainfall, flow discharge, sediment transport and cross-sectional profiles from the Taiwan Water Resources Agency are publicly available in the website (https://gweb.wra.gov.tw/wrhygis/ebooks/getebook.asp).

Received: 21 April 2025; Accepted: 12 June 2025; Published online: 23 June 2025

References

- 1. Davis, W. M. The geographical cycle. Geogr. J. 14, 481–504 (1899).
- 2. Thornbury, W. D. Principle of Geomorphology (John Willy, 1962).
- Knighton, D. Fluvial forms and Processes: A New Perspective (Hodder Education, 1997).
- Barko, V. A. & Schneider, J. R. Geomorphological effects of flow alteration on rivers. *River Syst. Environ. Manag.* 12, 245–263 (2016).
- Schumm, S. A. & Lichty, R. W. Time space and causality in geomorphology. Am. J. Sci. 263, 110–119 (1965).
- Lin, G.-W., Chen, H., Chen, Y.-H. & Horng, M.-J. Influence of typhoons and earthquakes on ranfall-induced landslides and suspended sediments discharge. *Eng. Geol.* 97, 32–41 (2008).
- Ho, J.-Y. & Lee, K. T. Performance evaluation of a physically-based model for shallow landslide prediction. *Landslides* 14, 961–980 (2017).
- 8. Huang, M. Y.-F. & Montgomery, D. R. Fluvial response to rapid episodic erosion by earthquake and typhoons. *Geomorphology* **175–176**, 126–138 (2012).
- Xu, C. et al. Optimized volume models of earthquake-triggered landslides. Sci. Rep. 6, 29797 (2016).
- Chang, J.-M., Chao, W.-A., Yang, C.-M. & Huang, M.-W. Coseismic and subsequent landslides of the 2024 Hualien earthquake (M7.2) on April 3 in Taiwan. *Landslides* 21, 2591–2595 (2024).
- Keefer, D. K. The importance of earthquake-induced landslides to long-term slope erosion and slope-failure hazards in seismically active regions. *Geomorphology*, 10, 265–284 (1994).
- Hartshorn, K., Hovius, N., Dade, W. B. & Slingerland, R. L. Climatedriven bedrock incision in an active mountain belt. *Science* 297, 2036–2038 (2002).
- Dadson, S. J. et al. Links between erosion, runoff variability and seismicity in the Taiwan orogeny. *Nature* 426, 648–651 (2003).
- Lin, C.-W., Liu, S.-H., Lee, S.-Y. & Liu, C.-C. Impacts of the Chi-Chi earthquake on subsequent rainfall-induced landslides in central Taiwan. Eng. Geol. 86, 87–101 (2006).
- Lee, C.-S. & Tsai, L. L. A quantitative analysis for geomorphic indices of longitudinal river profile: a case study of the Choushui River, central Taiwan. *Environ. Earth Sci.* 59, 1549–1558 (2010).
- Yanites, B., Tuckey, G. E., Mueller, K. J. & Chen, Y. G. How rivers react to large earthquakes: evidence from central Taiwan. *Geology* 38, 639–642 (2010).

- Hovious, N. et al. Prolonged seismically induced erosion and the mass balance of a large earthquake. Earth Planet. Sci. Lett. 304, 347–355 (2011).
- Cook, K. L., Turowski, J. M. & Hovius, N. River gorge eradication by downstream sweep erosion. *Nat. Geosci.* 7, 682–686 (2014).
- 19. Chen, H., Chen, R. H. & Lin, M. L. Initiative anatomy of Tungmen debris flow, eastern Taiwan. *Environ. Eng. Geosci.* **5**, 459–473 (1999).
- Chen, H. The geomorphological comparison of two debris flows and their triggering mechanisms. *Bull. Eng. Geol. Environ.* 58, 297–308 (2000).
- 21. Chen, H. Controlling factors of hazardous debris flow in Taiwan. *Quat. Int.* **147**, 3–15 (2006).
- 22. Chow, V. T. Handbook of Applied Hydrology (McGraw-Hill, 1964).
- 23. Lan, T. et al. Flow duration curve prediction: a framework integrating regionalization and copula model. *J. Hydrol.* **647**, 132364 (2025).
- 24. Lin, G. W., Chen, H., Shih, T. Y. & Lin, S. Various links between landslide debris and sediment flux during earthquake and rainstorm events. *J. Asian Earth Sci.* **54**, 41–48 (2012).
- Kuo, H. L. et al. Evaluating critical rainfall conditions for large-scale landslides by detecting event times from seismic records. *Nat. Hazards Earth Syst. Sci.* 18, 2877–2891 (2018).
- 26. Shen, Z.-M. Flow profile's preparation, debug and examination. *Taiwan Assoc. Hydraulic Eng. Sci.* **10**, 114–132 (1994). (in Chinese).
- Water Resources Agency. Guidelines for the surveying operations of the delineation and modification of centralized river areas (in Chinese) (2000).
- Water Resources Agency, Ministry of Economic Affairs. Hydrological Year Book of Taiwan, Republic of China (Water Resources Agency Ministry of Economic Affairs (in Chinese), 1990–2022).
- Liu, C. C. et al. Vicarious calibration of the formosat-2 remote sensing instrument. *IEEE Trans. Geosci. Remote Sens.* 48, 2162–2169 (2009).
- Liu, C. C., Shieh, C. L., Wu, C. A. & Shieh, M. L. Change detection of gravel mining on riverbeds from the multi-temporal and high-spatialresolution Formosat-2 imagery. *River Res. Appl.* 25, 1136–1152 (2009).
- Chang, C. H. et al. Monitoring reservoir water quality with Formosat-2 high spatiotemporal imagery. J. Environ. Monit. 11, 1982–1992 (2009).
- Liu, C. C. et al. Image processing of FORMOSAT-2 data for monitoring the South Asia tsunami. *Int. J. Remote Sens.* 28, 3093–3111 (2007).
- Liu, C. C. & Chen, P. L. Automatic extraction of ground control regions and orthorectification of remote sensing imagery. *Opt. Express* 17, 7970–7984 (2009).

Acknowledgements

This study has received funding from the Agency of Rural Development and Soil and Water Conservation, Taiwan. (Grant agreement no. ARDSWC-112-193) We thank the Taiwan Water Resources Agency, Geological Survey and Mining Management Agency, and the Agency of Rural Development and Soil and Water Conservation provide the measurement data.

Author contributions

J.-Y.H. and W.-L.L. Writing—original draft, validation, software, methodology, investigation, formal analysis, data curation, conceptualization. C.-H.L. and C.-H.C., Writing—review and editing, supervision, project administration. H.C., N.S., and Y.-C.C. Project administration and data curation

Competing interests

The authors declare no competing interests.

Additional information

Correspondence and requests for materials should be addressed to Jui-Yi Ho.

Reprints and permissions information is available at http://www.nature.com/reprints

Publisher's note Springer Nature remains neutral with regard to jurisdictional claims in published maps and institutional affiliations.

Open Access This article is licensed under a Creative Commons Attribution-NonCommercial-NoDerivatives 4.0 International License, which permits any non-commercial use, sharing, distribution and reproduction in any medium or format, as long as you give appropriate credit to the original author(s) and the source, provide a link to the Creative Commons licence, and indicate if you modified the licensed material. You do not have permission under this licence to share adapted material derived from this article or parts of it. The images or other third party material in this article are included in the article's Creative Commons licence, unless indicated otherwise in a credit line to the material. If material is not included in the article's Creative Commons licence and your intended use is not permitted by statutory regulation or exceeds the permitted use, you will need to obtain permission directly from the copyright holder. To view a copy of this licence, visit https://creativecommons.org/licenses/by-nc-nd/4.0/.

© The Author(s) 2025